

# MULTIPACTING IN 1400 MHZ BETA=0.5 CAVITIES FOR PROTON ACCELERATION

R. Ballantini\*, A.Chincarini, G. Gemme, R. Parodi, A. Podesta'  
 INFN\_Genoa, Via Dodecaneso 33, I-16146 Genova, Italy

## Abstract

The results of measurements on a prototype single cell  $\beta=0.5$  cavity are reported. The cavity operating at 1400 MHz was a scaled version (one fourth) of an early prototype of the cavities foreseen for the acceleration of intense proton beams. The cavity was built by deep drawing high RRR Niobium sheets 2 mm thick. The half cups, after a 200-micron BCP were EB-welded together and to the beam tubes at ZANON. The RF tests were performed after a 20-micron light BCP. The tests, performed @ 4.2 K, showed  $R_s = 400 \text{ n}\Omega$ , under 0.75 MV/m, corresponding to  $B_{\text{max}}=55$  Gauss, and the presence of a hard MP barrier upon this value causing a rapid but smooth drop of the  $Q_0$  value. Only after quite long Helium processing the barrier was overcome and the field reached the value of 14 MV/m. Measurements performed during the Helium processing revealed the presence of different MP barriers at different magnetic fields. The behaviour of the cavity was simulated using our TRAJECT code for Mp discharges simulation and a statistical analysis is computed. In the full paper the experimental results and the results of the simulations will be extensively compared.

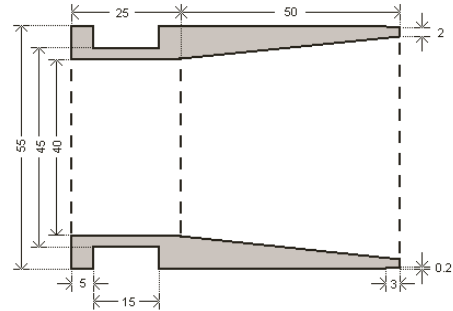


Figure 1: EB-welding drift tubes lathe made (Longitudinal section)

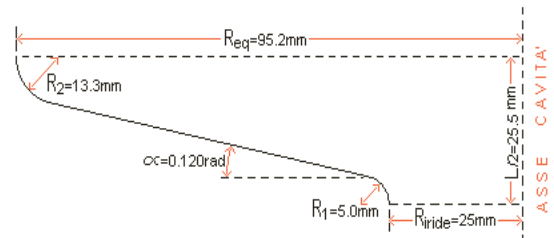


Figure 2: Half-cell made by deep drawing

## 1 CHARACTERISTICS OF THE CAVITY

The cavity, operating at 1400 MHz, is a scaled version (one fourth) of an early prototype of the cavities foreseen for the acceleration of intense proton beam at  $\beta=0.5$

The cavity was built by deep drawing high RRR niobium sheets 2 mm thick. The half cups, after a 200-micron BCP, were EB-welded together and to the beam tubes at ZANON. Using as normalization  $E_{\text{acc}}=1 \text{ MV/m}$  between the cavity irises, the electromagnetic properties of the cavity, calculated using our code OSCAR2D, are the following:

Table 1: cavity's characteristics

Resonant frequency	1406.5 MHz
Transit time factor	7.7590
Stored energy	$1.2093 \cdot 10^{-2} \text{ J}$
Voltage on the axis	65.300 KV/m
Max surface electric field	5.1934 MV/m
Max axial electric field	1.9566 MV/m
Max surface magnetic field	69.123 Gauss



Figure 3: Picture of the cavity

## 2 TREATMENTS AND MEASUREMENTS

### 2.1 RF tests after BCP treatment

The first RF tests were performed after a 20 micron light BCP. As a consequence of this treatment the maximum value of the secondary emission coefficient

\*renzo.ballantini@ge.infn.it

reaches values between 1.8 and 2.8. The tests, performed @ 4.2 K, showed  $R_s = 400 \text{ n}\Omega$  under  $0.75 \text{ MV/m}$ , corresponding to  $B_{\text{max}} = 55 \text{ Gauss}$ , and the presence of a hard MP barrier upon this value, causing a rapid but smooth drop of the  $Q_0$  value.

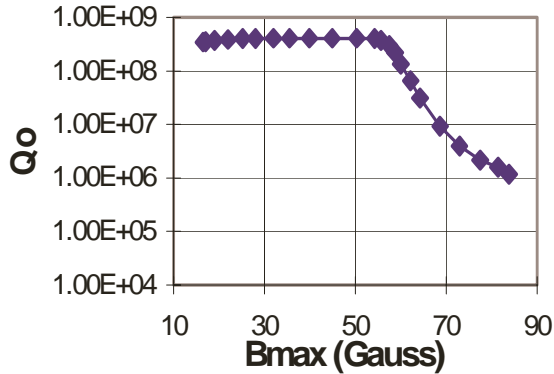


Figure 4:  $Q_0$  vs. maximum B field after light BCP.

The energy stored in the cavity, from a proportional relation with injected power, become a constant value and the  $Q_0$  crash down. The evidence of the MP barrier arose also analyzing the output power in square wave modulation.

### 2.2 RF tests during the Helium Processing.

To enhance its RF performances, the cavity was submitted to an helium processing, consisting in the injection of the maximum possible value of RF power (15 W) for several hours (10 in our case) in presence of rarefied gas. The ionised atom gas hurting the surface cause desorption of impurities. The result is the lowering of the secondary emission coefficient till its medium value is less then one.

A great vantage offered by using helium is that the treatment can be done @ liquid helium temperature with the cavity in superconducting state. The field intensity necessary to create the discharge can then be obtained injecting power inside the cavity from the same input antenna utilized for the measurements. In this way we can measure the resonator properties during and after the treatment without taking the cavity out from the cryostat, avoiding possible surface contaminations due to air exposition.

The helium pressure utilized during the treatment was  $10^{-5}$  mbar, the same used for LEP2 cavities.

The RF field utilized to give origin to the discharge corresponded to the fundamental one, in order to hit more intensively the region near the irises where surface irregularities create the best condition for electron field Emission. The helium ions hurt the cavity's surface with an energy from 10 KeV to several hundreds KeV.

The figure below shows the transmitted power (square wave) during the Helium Processing.

The process dynamics is the typical one of the relaxation discharge: inside the cavity the discharge is normal till the ionization field is reached, then the stored energy is rapidly consumed, the process ends and the charge starts again.

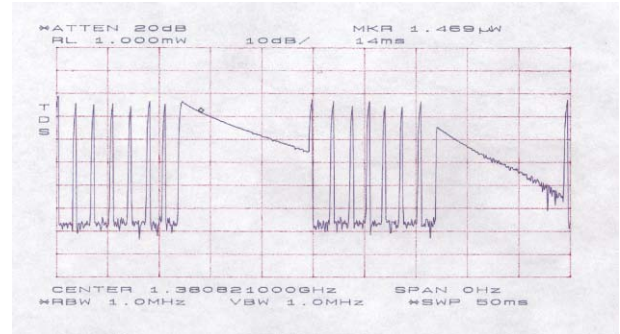


Figure 5: Transmitted power in square wave modulation during the Helium processing

A measure made after the first hour of Helium processing shows the presence of different MP barriers at different magnetic fields, as we can see in the following plot. The red line is the first measure and the blue one is the actual. The best accelerating field reached here is only  $2.8 \text{ MV/m}$

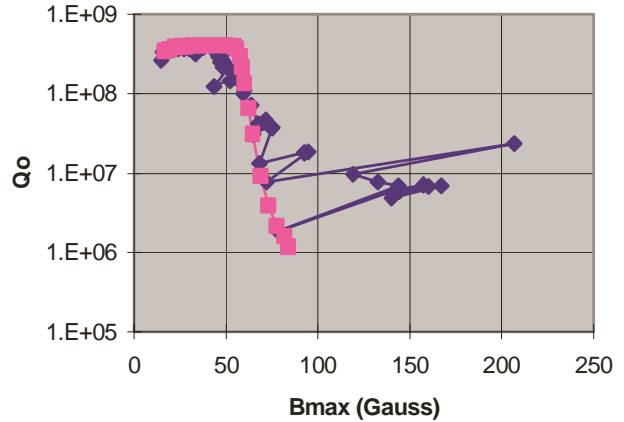


Figure 6:  $Q_0$  vs. max. B field during He processing

The comparison between these measures shows that during the H.P. treatment instead of the hard barrier of the first measure several soft barriers at greater fields were encountered. The nature of these barriers is put in evidence observing the output power vs. time in square wave modulation as shown in the following plot.

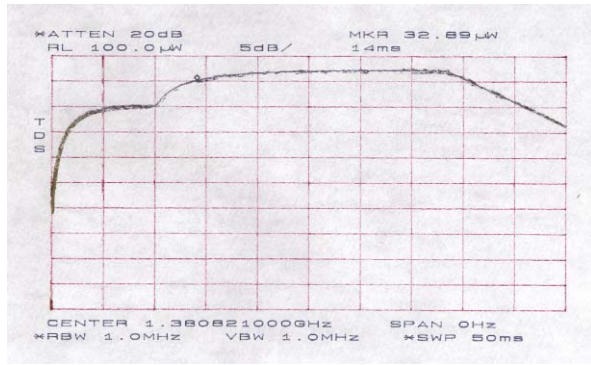


Figure 7: Transmitted power in square wave Modulation after 1 hour H.P. at a field corresponding to an MP barrier.

### 2.3 RF tests after The Helium Processing

The barrier was definitively overcome only after 10 hours Helium processing. The tests @ 4.2 K after this treatment showed no MP barrier up to 12 MV/m accelerating field,  $R_s \gg 200 \text{ n}\Omega$  and a maximum accelerating field around 14 MV/m. The  $Q_0$  profile is nearly flat, except for the initial growth at low fields due to noise. Soft MP barriers are still present in the field region between 12 and 14 MV/m.

We show here the  $Q_0$  vs.  $B_{\text{peak}}$  because of the typical direct dependence of MP on its value (synchronization conditions).

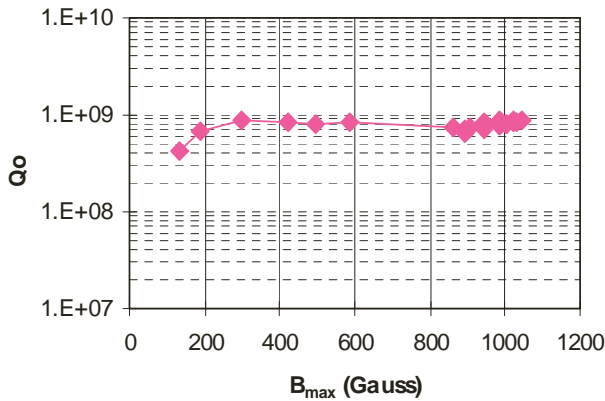


Figure 8:  $Q_0$  vs. the peak magnetic field after about 10 Hours of Helium Processing.

## 3 SIMULATIONS

The RF behaviour of the cavity was simulated using TW-TRAJ code [1] developed to study multipacting phenomenon in SRF cavities. Extensive simulations were made supposing values of the secondary emission coefficient  $\delta$ : 2.2 (Nb after BCP), 1.5 (baked Nb) [2] and 1.25 (Nb after Helium processing). Sweeping the fields in the interval from zero to 1300 Gauss at steps of 5 and 10 Gauss, under and over 350 Gauss respectively, a statistical analysis were made in the following way: at each field, the trajectories of 800 electrons starting from the equatorial region of the cavity and the yield at each

impact are computed. For each of these electrons the average life (in # of impacts) is taken into account. The mean yield per impact and the mean impact energy are calculated from the simulated trajectories reaching a fixed number of impacts. An effective growth rate per impact of the number of electrons in the cavity is then computed.

### 3.1 MP barrier calculation

B field values at which MP barriers could arise are calculated establishing synchronization conditions between particles and RF field. Using first order correction for the effective field, this gives:

$$\text{for 1 point multipacting} \quad B = \frac{280}{n} \left[ \frac{\text{Gauss}}{\text{GHz}} \right] \nu$$

$$\text{for 2 points multipacting} \quad B = \frac{560}{2n-1} \left[ \frac{\text{Gauss}}{\text{GHz}} \right] \nu$$

Despite the fact that inside the cavity the fields change from point to point, this rule gives a single B field value, according to the characteristic that multipacting arise in cavity's regions where B field is almost uniform and close to its maximum value. For 1400 MHz cavities this rule gives the following values for the magnetic field corresponding to the first four MP level orders:

Table 2: B field values corresponding to MP barriers

Level order	MP 1pt	MP 2pt
1	392	784
2	196	261
3	131	157
4	98	112

The synchronism condition is necessary but not sufficient for the presence of MP barriers: multipacting phenomenon arises when the electromagnetic field makes stable electron trajectories possible, with enough electrons energy and impact angles to have a secondary emission coefficient greater than one. Due to this fact, the analysis technique must take into account the number of impacts, the growth rate of electrons inside the cavity and the total yield for each electron.

### 3.2 Average life

The average electrons life, given in terms of number of impacts, for the 1400 MHz cavity's geometry is shown in figure 9. The simulations reveal that in quite large range of B field, centered at 750 Gauss, the electrons reach a

great number of impacts. This is in agreement with the value corresponding to the first level order of 2 point multipacting.

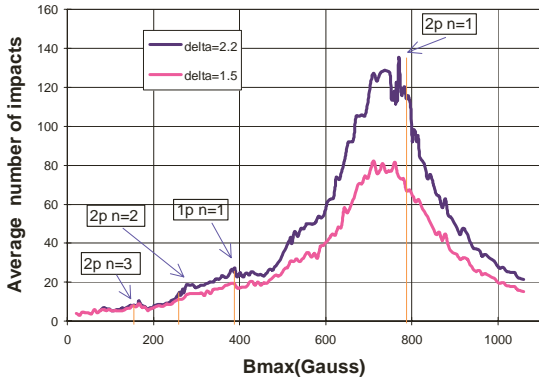


Figure 9: Secondary emission process growth rate plot.

### 3.3 Growth rate calculation

The main number of secondary electrons generated by a simulated primary one and surviving the  $N^{th}$  impacts is:

$$S = \prod_{i=1..N} \delta_i - 1$$

So their number grows  $S^{1/N}$  times at every impact. The growth of the number of electrons per impact is then the average of this number over all the simulated processes. We estimated this rate considering R: the calculated mean yield (for  $\delta$ ), and mean life (for N), calling  $\Delta$  this average growth rate.

$$\Delta = \sqrt[N]{R^N} - 1$$

The vertical lines in the plot indicate the B fields corresponding to synchronous conditions.

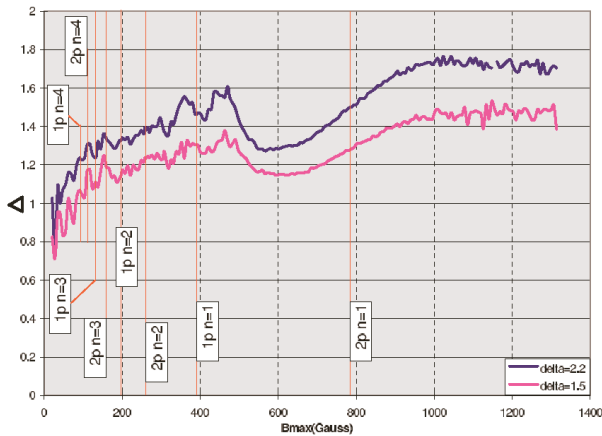


Figure 10: Growth rate plot.

The curves shown in figure 10 can be subdivided in four parts: the first one below 100 Gauss where the average growth is less than unity, the second zone up to

500 Gauss where peaks much more greater than the unity arise, a third area up to 700 Gauss with low growth values and the last zone above 700 Gauss where the average growth increases again. According to this analysis the simulation predicts a dangerous zone at low B field: the second one. If this zone could be surmounted then no MP problem were encountered up to 800 Gauss, corresponding to 12 MV/m accelerating field.

### 3.4 Yield Analysis.

For a maximum number of impacts equal to 10 we can observe relative peaks well corresponding to the fields satisfying synchronization condition.

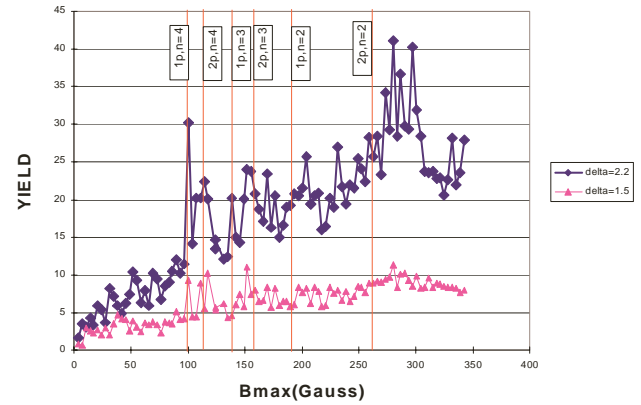


Figure 11: mean yield at 10 impacts vs. B field.

Comparison of the mean yield between simulations stopped at 10 and 50 impacts: the larger fluctuations of the 50 impacts simulations are due to bigger statistical fluctuations. For high fields the correspondence among the maximum values of the main yield and synchronization condition is not anymore good.

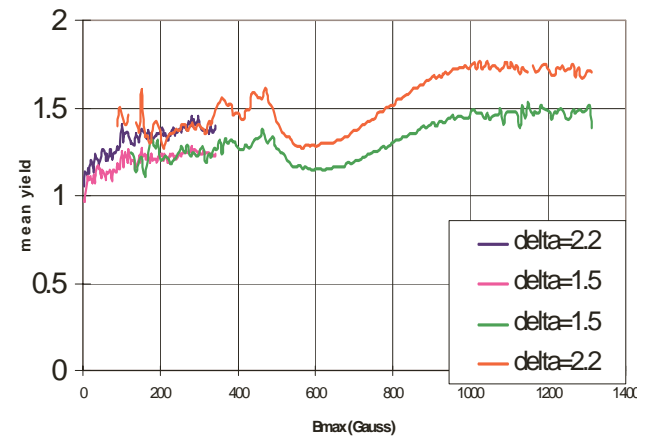


Figure 12: comparison between mean yield at 10 and 50 impacts

## 4 CONCLUSIONS

The barrier in the first measurements is found where the simulated growth rate crosses the value 1. Simulations with  $\delta_{max} = 1.25$  show no value of  $\Delta$  greater than 1 at low

fields, and no barrier is found. We can see irregularities in the  $Q_0$  line just at high fields just where  $\Delta$  surpasses one. The value of  $\Delta$  vs.  $B$  in simulations with  $\delta_{max}= 2.2$  (Nb after BCP) and 1.25 (Nb after He-processing) are here reported and put in comparison with experimental results of  $Q_0$  in the first (brown line) and in the last (violet) measurements.

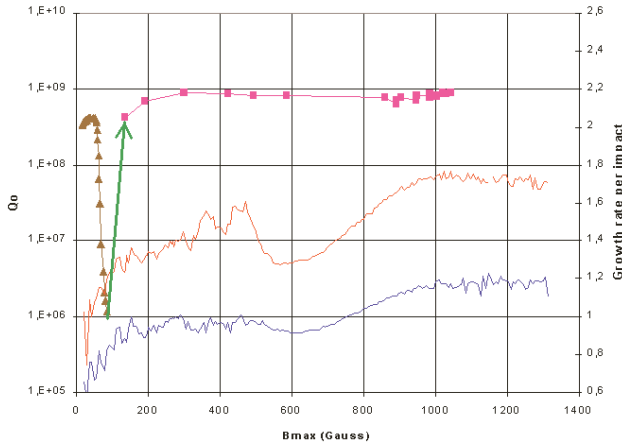


Figure 13: Comparison between tests and simulations.

According to our analysis method, what is expected is not an exact correspondence between the minimum  $Q_0$  values and maximum  $\Delta$  values but to observe a  $Q_0$  drop for those values of magnetic field for which  $\Delta$  is greater than one. This first  $\beta=0.5$  cavity reveals multipacting problems: not surmountable MP barriers are present at very low fields, and can be surpassed only keeping the secondary emission coefficient at the lowest possible values.

Simulations foresee relative maxima in mean yield and mean life of the trajectories at the fields foreseen by synchronization conditions. These peaks are thin spikes upon a wide smooth hill, followed by a valley of relatively low MP risk.

The effectiveness of different treatments in overcoming the soft MP barriers and in increasing RF cavity's performances will be further tested on a new cavity prototype, with the same geometry and characteristics, built and polished at CERN SL-Division (courtesy E. Chiaveri).

## 5 ACKNOWLEDGMENTS

We thank O. Aberle, A. Insomby and E. Chiaveri for the realization of the new 1400 MHz cavity prepared at CERN and R. Losito for his precious suggestions about Helium Processing treatment.

## 6 REFERENCES

- [1] P.Fernandes, R.Parodi, "NEWTRAJ, A COMPUTER CODE FOR THE SIMULATION OF THE ELECTRON DISCHARGE IN ACCELERATING STRUCTURES", Proceedings of "Particles accelerator conference" Ieee catalog 89CH2387-9 edited By R.Lindstrom and Louise Taylor. Washington DC 16-19 Marzo 1987.pag-1857
- [2] R.Boni, V.Chimenti, P.Fernandes, R.Parodi, B.Spataro, F.Tazioli: "REDUCTION OF MULTIPACTORING IN AN ACCELERATOR CAVITY", IEEE Transaction on Nuclear Science, October 1998